



Получена: 12.02.2018 г.

Приета: 27.03.2018 г.

STRESS-DEFORMED CONDITION OF CORROSION DAMAGED REINFORCED CONCRETE MEMBER UNDER DYNAMIC LOADING

A. Tamrazyan¹, D. Popov²

Keywords: reinforced concrete element, corrosion damage, dynamic loading, load bearing capacity

ABSTRACT

Using modern computing software complex Lira 10.6, a comparative evaluation of the undamaged and the corrosion-damaged reinforced concrete elements under dynamic and static loading is carried out. The influence of the weakened by corrosion concrete part of the compressed area on the redistribution of stresses in the section is analyzed.

1. Introduction

Exposure to aggressive environments results in corrosion processes that cause significant degradation of the load bearing capacity of reinforced concrete elements of buildings and constructions during their operation [1]. Long-term operation without taking measures to overhaul leads to a decrease in structural safety and durability of buildings. Targets for the reduction of load bearing capacity during beyond design basis effects and as a consequence, predicting the risks of collapse of structures and buildings is essential to ensure the safety of building structures [2 – 4].

¹ A. Tamrazyan, Prof, Dr Tech. Sc, National Research Moscow State University of Civil Engineering, Moscow, Russia, e-mail: tamrazian@mail.ru

² D. Popov, Assoc., National Research Moscow State University of Civil Engineering, Moscow, Russia, e-mail: popovds89@mail.ru

2. Formulation of Problem

At the present stage of scientific activity, data on the calculation principles, the level of stresses and strains arising in the corrosion-damaged reinforced concrete elements under dynamic loading are insufficient.

The aim of this work is to determine the stress-strain state of the corrosion-damaged bending beam, to define the displacement, to describe the impact of the weakened concrete part on the redistribution of stresses in the section under dynamic loading element.

3. Method of Solving the Problem

To determine the deflected mode along the entire section of the element with its corrosive damage, the reinforced concrete beam is modelled with the help of three-dimensional 8-node finite elements. Concrete is made of finite elements with the size of $25 \times 25 \times 50$ mm, reinforcement is $20 \times 12,7 \times 50$ mm, which corresponds to the equivalent area of reinforcement with a diameter of 18 mm.

The adopted reinforced concrete beam is 2,0 m length, 0,3 m width, 0,6 m height and reinforced with two rods of 18 mm in diameter in the tensile section area.

Based on the principles of given rigidities, the linear isotropic materials are accepted, where a concrete class is B25 with an elastic modulus $E_b = 30 \times 10^3$ MPa, reinforcement class is A400 with modulus of elasticity $E_s = 2 \times 10^5$ MPa.

The result of constant exposure of the reinforced concrete to aggressive environments is corrosion damages of reinforcement and concrete. In consequence of that there is a decrease in the strength characteristics of materials. In this case corrosion damage is modelled in the average in length part of the beam. The damage in focus is taken by the size $0,5 \times 0,3 \times 0,11$ m (Fig. 1). Strength characteristics of the damaged concrete part of the section are adopted with modulus of elasticity $E_b = 10 \times 10^3$ MPa that corresponds to the concrete class B5.

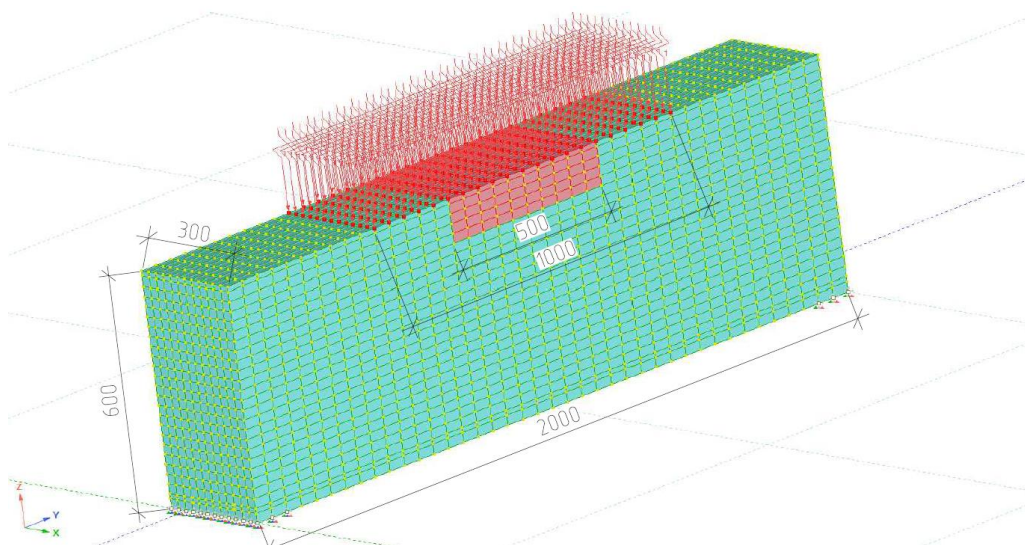


Figure 1. The model of the concrete corrosion-damaged beam under dynamic impact

The reinforced concrete element is exposed to two static loads: self-weight and a uniformly distributed load of intensity 40 t/m^2 . It is also subjected to a dynamic load, modelled by the impact in the middle part of a beam span with the size of $1,0 \text{ m}$. There is a single impact attached at the speed of $0,04 \text{ sec.}$ and intensity of $1,0 \text{ t}$ (Fig. 1). The applied dynamic load can occur for the cause of the collapse of the overlying slab in the result of an emergency situation.

Calculation of dynamic load was performed using the module "Dynamics +". This module allows to evaluate the deflected mode in the target time period, and to determine at what time period there are the maximum tensile and compressive stresses in the three-dimensional finite elements.

The dynamic calculation was done with the use of modal analysis which allows to determine the forms and frequencies of natural vibrations of the structure. The first and the second mode shape were adopted according to the results of the modal analysis, respectively $102,81 \text{ Deg/s}$ and $230,15 \text{ Deg/s}$ of the natural vibration frequency, which in turn is necessary while taking into account the damping.

The formation of mass matrixes for dynamic loading is made of static load cases. To analyze the deflected mode at the moment and after application of the impact load, the period of fixing the stresses and strains of 5 seconds was adopted.

Maximum normal stresses N_x, N_y, N_z occur at the moment of impact ($0,04 \text{ s}$). For clarity, there are the graphs of maximum tensile (+ sign) and compressive (- sign) stress within the definite time period for three-dimensional finite element "concrete" (Fig. 2 – 4) located in the compressed part of the section and three-dimensional finite element "reinforcement" located in the tensile section (Fig. 5 – 7). The considered finite elements are in the middle section, where there is the maximum stress relative to the entire beam. These finite elements, like the reinforced concrete beam in general, have initial mechanical characteristics of the material (without corrosion damage).

Having analyzed the graphs of normal stresses in the three-dimensional finite element "concrete" it can be concluded that the maximum compressive stresses N_y, N_z occur at $0,04 \text{ second}$, when the peak of the impact load happens, whereas the extreme tensile stress is observed at $0,066 \text{ second}$. The stresses N_x arising at $0,04 \text{ second}$ are tensile, while the stresses at $0,066 \text{ second}$ are compressive.

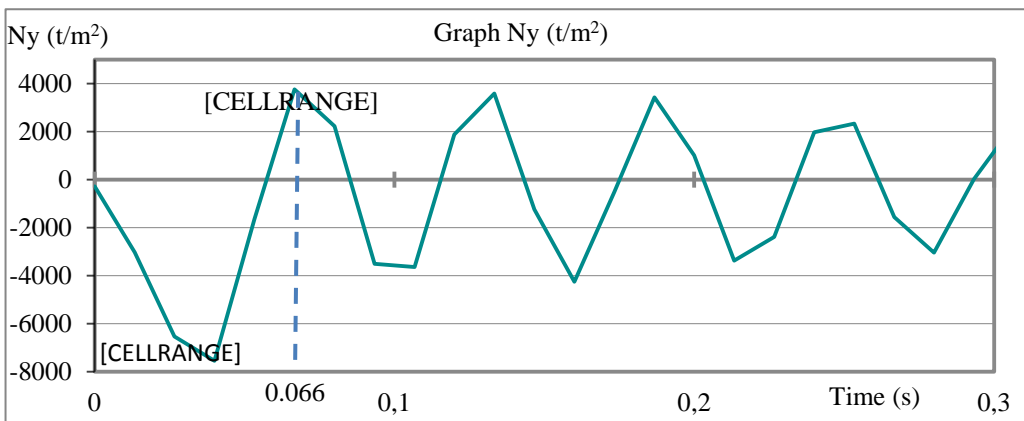


Figure 2. The normal stresses N_y in the three-dimensional finite element "concrete"

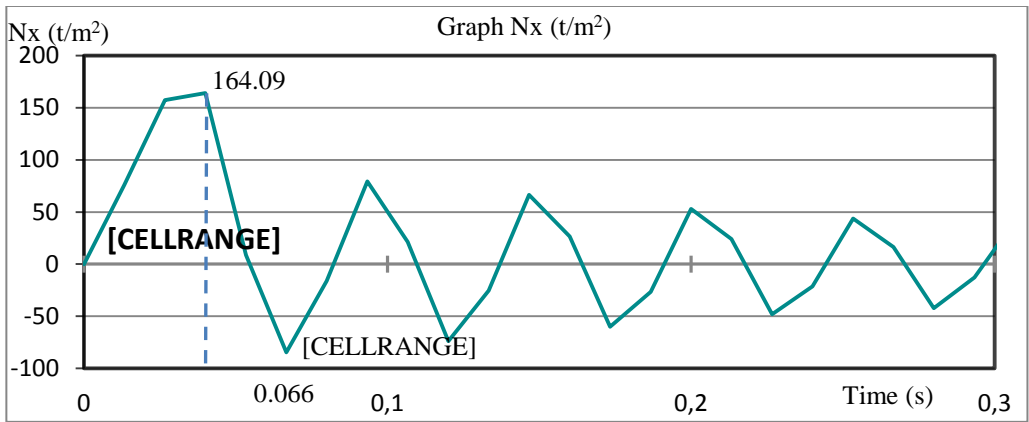


Figure 3. The Normal stresses N_x in the three-dimensional finite element “concrete”

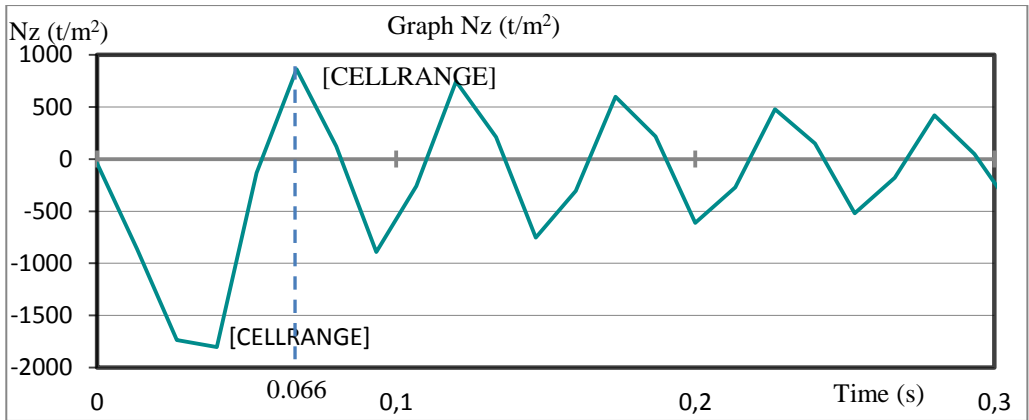


Figure 4. The normal stresses N_z in the three-dimensional finite element “concrete”

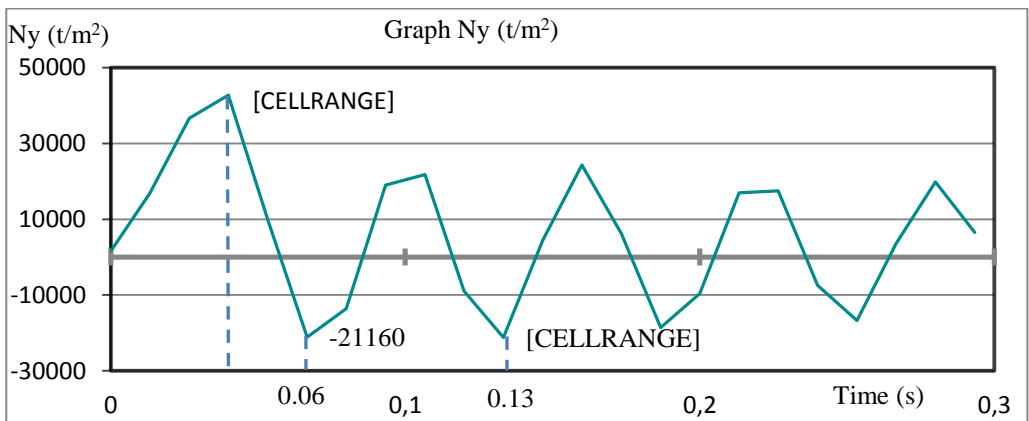


Figure 5. The normal stresses N_y in the three-dimensional finite element “reinforcement”

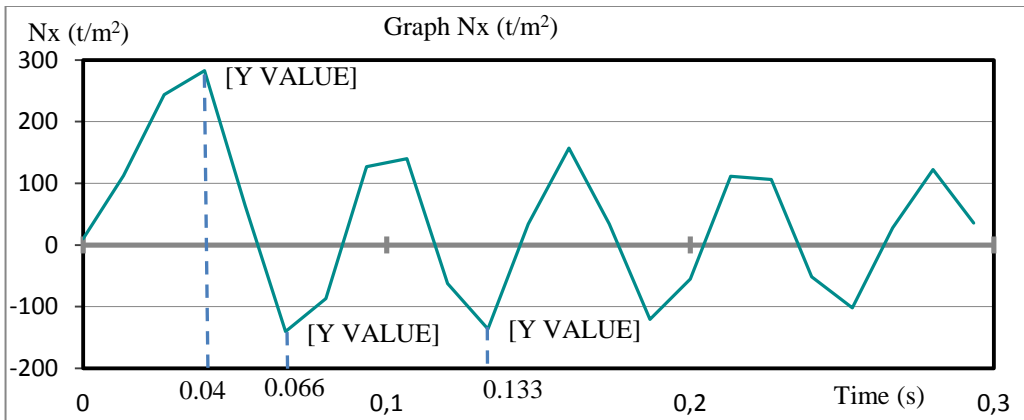


Figure 6. The normal stresses N_x in the three-dimensional finite element “reinforcement”

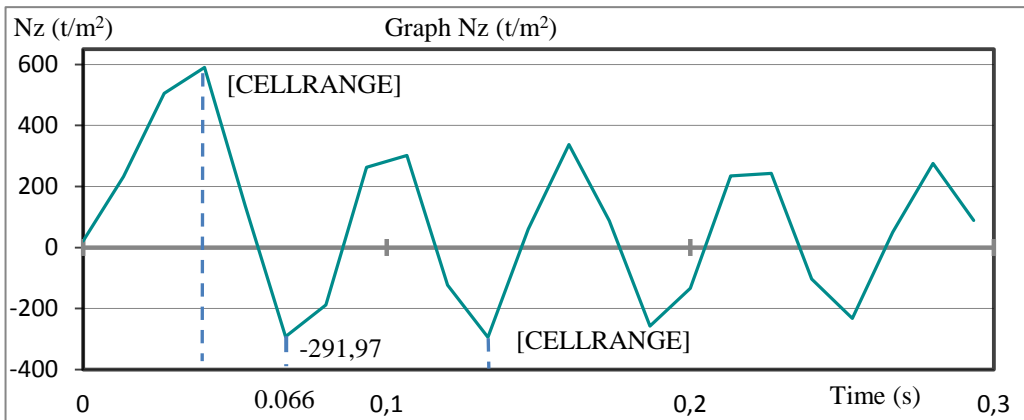


Figure 7. The normal stresses N_z in the three-dimensional finite element “reinforcement”

Fig. 8 shows stress plots in the middle section of reinforced concrete bending beams from a static load. In the section, compressive and tensile stresses N_y directed perpendicular to the normal section of the element are considered. The cross section of the "A" element is not damaged, in the extreme compressed concrete fiber there are stresses equal to $\sigma_b = 2,7$ MPa, in the extreme stretched concrete fiber $\sigma_{bt} = 2,7$ MPa, and the stresses arising in the tensile reinforcement $\sigma_s = 15,87$ MPa. The cross section of the "B" element is a partially corroded reinforced concrete element in the compressed section area (see Fig. 1), where the stresses occurring in the corroded damaged final compressed concrete fiber are $\sigma_b = 1,6$ MPa, in the extreme stretched concrete fiber $\sigma_{bt} = 3,04$ MPa, and the stresses arising in the stretched armature $\sigma_s = 18,3$ MPa. From the values obtained, it is noted that in the damaged element "B" the tensile stresses are greater than in the undamaged element, but the resulting compressive stresses in the compressed corrosion-damaged region of the "B" element are smaller.

This fact can be explained by the fact that the strength characteristics of the encoded section decreased, thereby the constant operating stresses from the external load are redistributed, increasing in the tensile part of the section.

The distribution of the normal stresses in the compressed part of the section of corrosion-damaged element has an abrupt shape, the increase of stress occurs at the boundary of damaged and undamaged concrete (Fig. 8).

In his work [6] a scheme of the stress condition of the normal cross-section of corrosion-damaged elements is given (Fig. 9).

Fig. 9 indicates A as an area of full corrosion concrete cracking (z^*); B is an area of partial corrosion damage to the concrete (δ); B is an area of undamaged concrete (p); a, b, x^*, h, h_0 are the geometrical sizes of the concrete body (sample); K^* is a curve function damage (retention of the original mechanical characteristics); Fz^* is the value of the lost part of the power resistance, caused by the destruction of the area A ; F_1 is the value of the lost part of the power resistance, due to lower power resistance in the area B ; F_2 is the value of the remaining part of the power resistance in the area B ; F_s is the value of the power resistance of the corroded design reinforcement A_{s0} ; ω_s is the coefficient of the reinforcement corrosion damage.

4. Calculation and Results

Omitting the calculations of the work [5], the remaining resistance forces in the reinforced concrete elements are of the form:

$$F_s = \omega_s A_s R_s; \quad F_2 = b R_b \int_0^{\delta} k dz = \frac{2}{3} b \delta z = \frac{2}{3} b \delta R_b; \quad F_n = b p R_b. \quad (1)$$

Instant arms of force F_2 and F_n , relative to the center of gravity of the tensile reinforcement:

$$r_{s,2} = h_0 - \left(z^* + \frac{5}{8} \delta \right); \quad r_{s,n} = h_0 - \left(z^* + \delta + \frac{1}{2} p \right). \quad (2)$$

The limit bending moment of power resistance in the section with a glance to corrosion damage

$$M_{np}^* = F_2 r_{s,2} + F_n r_{s,n}. \quad (3)$$

The height of the compressed area of the corrosion – damaged element

$$x^* = x + z^* + \frac{1}{3} \delta. \quad (4)$$

The height of the undamaged concrete of the compression area:

$$p = x^* - (z^* + \delta). \quad (5)$$

Let us determine the limit bending moment according to (1 – 5), with the conditions: $x = 30,3$ cm and $\delta = 11$ cm (Fig. 8); $b = 30$ cm; $h_0 = 57$ cm; $z^* = 0$; $\omega_s = 1$, concrete class B25, $R_b = 14,5$ MPa:

$$x^* = 30,3 + 11/3 = 33,9 \text{ cm}. \quad (6)$$

$$p = 33,9 - 11 = 22,9 \text{ cm}. \quad (7)$$

$$M_{np}^* = \frac{2}{3} 30 \cdot 11 \cdot 1,45 \left(57 - \frac{5}{8} 11 \right) + 30 \cdot 22,9 \cdot 1,45 (57 - 11 - 22,9/2) = 50406,8 \text{ kN/cm}. \quad (8)$$

Let us define M_{np}^* [7] including partial corrosion damage in the compressed area of concrete according to the conditions: $\delta = 11$ cm with a design compressive strength $R_b^* = 2,8$ MPa (class B5); the strength of the intact concrete $R_b = 14,5$ MPa (class B25); the height of the compressed area of the corrosion-damaged element $x^* = 32,7$ cm (Fig. 8); $h_0 = 57$ cm; $b = 30$ cm.

$$M_{np}^* = R_b^* b \delta (h_0 - \delta / 2) + R_b b (x^* - \delta) \left(h_0 - \frac{x^* - \delta}{2} \right);$$

$$M_{np}^* = 0,28 \cdot 30 \cdot 11 \cdot (57 - 11 / 2) + 1,45 \cdot 30 (32,7 - 11) \left(57 - \frac{32,7 - 11}{2} \right) = 48321,9 \text{ kN/cm.} \quad (9)$$

When comparing the criteria for finding the limit bending moment, we can say that in the work [5], in the compressed area of concrete Б (Fig. 9), 1/3 of the area of corrosion-damaged concrete is excluded (δ), the preserved concrete area is taken with the original strength characteristics and is multiplied by the corresponding arms of force to the centre of gravity of the tensile reinforcement, the height of the compressed area is determined by the work (4). In the work [7] the area of the corrosion-damaged compressed concrete area Б (Fig. 9) does not change, but it is taken into account with the reduced strength characteristics, and the height of the compressed area is determined from the data and software complex (Fig. 8).

In addition to the reducing of the load bearing capacity of the reinforced concrete element due to the corrosion processes, there is a risk of brittle fracture, due to the increased height of the compressed area that happens in case of non-fulfilment of the conditions:

$$\xi = \frac{x}{h_0} \leq \xi_R. \quad (10)$$

where ξ is the relative height of the compressed area, ξ_R is the ultimate relative height of the compressed area, the value of which depends on the class of the reinforcement; x is the height of the compressed zone; h_0 is the effective depth of section.

Let us verify the condition (10) for the corrosion-damaged element according to [5], where $\xi_R = 0,531$ corresponds to the reinforcement class A400.

$$\xi = \frac{32,7}{57} = 0,573 \geq \xi_R = 0,531. \quad (11)$$

The condition (10) is not met; therefore, brittle fracture of the element will occur.

Stresses $\sigma_1, \sigma_2, \sigma_3$ are a special case of the normal stresses, they act at the main sites. Normal stresses N_y, N_z, N_x , on the main sites take extreme values.

For three-dimensional finite elements, No. 1 – 3, located in the compressed area of section of the corrosion-damaged and undamaged element (Fig. 8), the basic stresses and their corresponding deformations are given in Tables 1 and 2 in the dynamic and the static arrangement accordingly.

Table 1. The basic stresses and their corresponding strains under dynamic loading

Undamaged three-dimensional finite elements														
№	σ_1 min (t/m ²)	σ_1 max (t/m ²)	σ_2 min (t/m ²)	σ_2 max (t/m ²)	σ_3 min (t/m ²)	σ_3 max (t/m ²)	τ min (t/m ²)	τ max (t/m ²)	ϵ_1 min	ϵ_1 max	ϵ_2 min	ϵ_2 max	ϵ_3 min	ϵ_3 max
1	-41.175	2776.7	-1228.2	609.49	-5559	20.309	103.08	2758.9	1.60E-05	8.66E-04	-5.32E-05	1.07E-04	-1.73E-03	-6.49E-05
2	-25.949	3109.5	-1180.1	584.53	-6224.8	-22.588	115.62	3134.9	1.76E-05	9.79E-04	-6.24E-05	1.18E-04	-1.96E-03	-7.31E-05
3	-54.522	3453	-1191.3	589.84	-6911.7	-45.335	128.23	3501.9	1.93E-05	1.09E-03	-7.28E-05	1.33E-04	-2.19E-03	-8.03E-05
Damaged three-dimensional finite elements														
1	-98.783	1851.3	-1346.7	668.16	-3442.1	48.756	61.302	1671.7	2.96E-05	1.64E-03	-6.02E-04	2.97E-04	-2.97E-03	-1.09E-04
2	-28.817	2072.2	-1227.3	607.2	-3810.7	26.163	68.833	1910.2	3.28E-05	1.86E-03	-4.41E-04	2.24E-04	-3.37E-03	-1.23E-04
3	-11.518	2267	-1224.1	605.74	-4137.6	-8.4975	75.55	2118.8	3.63E-05	2.05E-03	-3.93E-04	2.35E-04	-3.69E-03	-1.35E-04

Table 2. The basic stresses and their corresponding strains under static loading

Undamaged three-dimensional finite elements							
№	σ_1 (t/m ²)	σ_2 (t/m ²)	σ_3 (t/m ²)	τ (t/m ²)	ϵ_1	ϵ_2	ϵ_3
1	-0.041	-38.324	-206.200	103.080	1.60E-05	9.55E-07	-6.49E-05
2	-0.200	-39.237	-231.450	115.620	1.76E-05	2.32E-06	-7.31E-05
3	-0.244	-39.835	-256.690	128.230	1.93E-05	3.78E-06	-8.13E-05
Damaged three-dimensional finite elements							
№	σ_1 (t/m ²)	σ_2 (t/m ²)	σ_3 (t/m ²)	τ (t/m ²)	ϵ_1	ϵ_2	ϵ_3
1	-1.890	-42.039	-124.490	61.302	2.96E-05	-1.58E-05	-1.09E-04
2	-1.141	-40.666	-138.810	68.833	3.28E-05	-1.20E-05	-1.23E-04
3	0.254	-40.431	-150.850	75.550	3.63E-05	-9.73E-06	-1.35E-04

Comparing the current maximum and minimum basic stresses and their corresponding strains in static and dynamic arrangement, it can be concluded that the appearing strains in the corrosion-damaged three-dimensional finite elements happen more often than in undamaged ones, despite the fact that some of the operating basic stresses in the same KE happen more occasionally.

For three-dimensional finite elements No. 4 – 7 (Fig. 8) in the Tables 3 and 4 the basic stresses and strains in static and dynamic arrangement respectively are given. KE are taken undamaged, but the definition of maximum and minimum basic stresses and their corresponding strains are formed from the damaged and undamaged reinforced concrete beam.

Table 3. The basic stresses and their corresponding strains under dynamic loading

Undamaged reinforced concrete element														
№	σ_1 min (t/m ²)	σ_1 max (t/m ²)	σ_2 min (t/m ²)	σ_2 max (t/m ²)	σ_3 min (t/m ²)	σ_3 max (t/m ²)	τ min (t/m ²)	τ max (t/m ²)	ϵ_1 min	ϵ_1 max	ϵ_2 min	ϵ_2 max	ϵ_3 min	ϵ_3 max
4	-139.86	42709	-291.42	589.33	-21121	282.36	788.5	21213	7.9E-05	2.1E-03	-6.2E-04	3.0E-04	-1.0E-03	-2.4E-05
5	84.162	3460.5	-1.0248	0.5058	-1751.9	-6.3074	67.455	1844	4.2E-05	1.1E-03	-2.1E-04	1.1E-04	-5.8E-04	-1.0E-05
6	-11.179	869.97	-558.32	277.8	-897.05	5.5436	13.213	631.21	3.1E-06	3.1E-04	-1.3E-04	6.3E-05	-3.1E-04	-7.3E-06
7	-8.1326	1574.7	-1076.7	535.19	-3000.9	4.0369	56.293	1496.4	9.4E-06	4.9E-04	-1.6E-04	7.6E-05	-9.1E-04	-3.5E-05
Damaged reinforced concrete element														
№	σ_1 min (t/m ²)	σ_1 max (t/m ²)	σ_2 min (t/m ²)	σ_2 max (t/m ²)	σ_3 min (t/m ²)	σ_3 max (t/m ²)	τ min (t/m ²)	τ max (t/m ²)	ϵ_1 min	ϵ_1 max	ϵ_2 min	ϵ_2 max	ϵ_3 min	ϵ_3 max
4	-178.7	49837	-362.31	687.1	-26231	346.07	908.51	24745	9.1E-05	2.5E-03	-7.2E-04	3.8E-04	-1.3E-03	-2.7E-05
5	49.507	3691.4	-2.9247	1.4506	-1975.2	-11.564	73.565	2032.6	4.5E-05	1.2E-03	-2.2E-04	1.2E-04	-6.6E-04	-1.3E-05
6	-17.309	1152	-1069.6	532.53	-1764.5	8.696	32.665	873.59	6.5E-06	3.5E-04	-2.3E-04	1.2E-04	-5.1E-04	-1.9E-05
7	-0.603	2788.3	-1461.3	727.67	-5220.3	0.3066	96.325	2609.9	1.6E-05	8.8E-04	-1.4E-04	9.1E-05	-1.6E-03	-6.0E-05

Table 4. The basic stresses and their corresponding strains under static loading

Undamaged reinforced concrete element							
№	σ_1 (t/m ²)	σ_2 (t/m ²)	σ_3 (t/m ²)	τ (t/m ²)	ϵ_2	ϵ_3	σ_1 (t/m ²)
4	1587.2	21.985	10.215	788.5	7.89E-05	-2.3E-05	-2.4E-05
5	128.6	-0.03697	-6.3074	67.455	4.24E-05	-8E-06	-1E-05
6	0.028957	-20.85	-26.397	13.213	3.1E-06	-5.1E-06	-7.3E-06
7	-0.00548	-31.703	-112.59	56.293	9.43E-06	-3E-06	-3.5E-05
Damaged reinforced concrete element							
№	σ_1 (t/m ²)	σ_2 (t/m ²)	σ_3 (t/m ²)	τ (t/m ²)	ϵ_2	ϵ_3	σ_1 (t/m ²)
4	1829.4	25.304	12.43	908.51	9.09E-05	-2.6E-05	-2.7E-05
5	135.57	-0.08293	-11.564	73.565	4.51E-05	-8.1E-06	-1.3E-05
6	-0.07985	-34.519	-65.409	32.665	6.51E-06	-7E-06	-1.9E-05
7	0.1967	-44.557	-192.45	96.325	1.56E-05	-2E-06	-6E-05

Comparing the data of the Tables 3 and 4, it is determined that the maximum and minimum basic stresses and their corresponding strains appear in the undamaged three-dimensional finite elements of the corrosion-damaged beam. This is because the strength characteristics of corrosion-damaged finite elements are reduced with respect to the original ones, resulting in redistribution of the operating stresses from external loads on the mating parts, increasing their numbers.

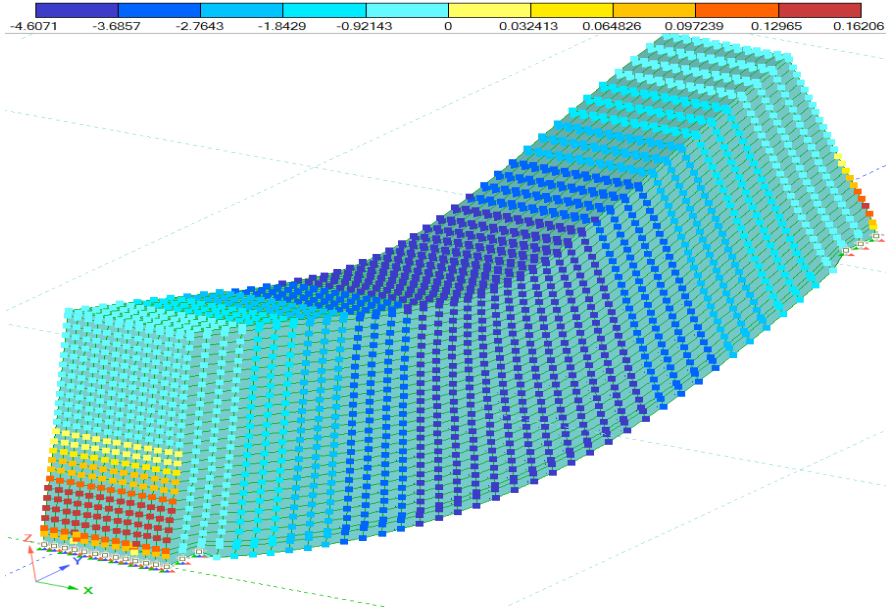


Figure 10. The Z-axis displacement of the corrosion-damaged reinforced concrete beam

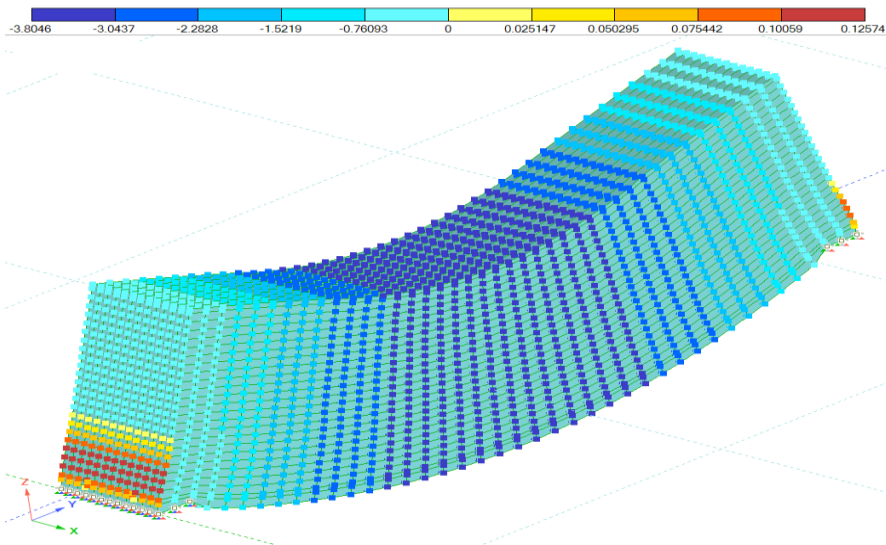


Figure 11. The Z-axis displacement of the undamaged reinforced concrete beam

In addition to the emerging stresses and strains from external loads, there are moving nodes along the local axes Z , X , Y . Fig. 10 and 11 show the total displacement along the Z axis from dynamic loading, the undamaged and corrosion-damaged reinforced concrete element, respectively.

5. Conclusions

Maximum displacements of nodes along the Z -axis occur at 0,066 second, the displacement of the nodes of corrosion-damaged element is more than 0,8 mm, which is 17%. The cause of large displacements is smaller rigidity of the corrosion-damaged beam.

Thus, the conclusions based on the results of the calculation in the software package, corrosion-damaged and undamaged beams of three-dimensional 8-node finite elements are:

- corrosion-damaged beam stresses in the tensile area are larger, and the stresses in the compressed area are smaller than in the undamaged beam;
- the risk of brittle fracture of the corrosion-damaged element increases, due to the increased height of the compressed area of concrete;
- in the corrosion-damaged KE under dynamic and static loading the appearing strains are larger than in the undamaged ones, even assuming that some of the operating basic stresses in the same KE are smaller;
- due to the redistribution of efforts in undamaged FE corrosion-damaged beams, appearing stresses and the corresponding strains are larger than in the undamaged beam.

REFERENCES

1. *Larionov, E. A.* Influence of Corrosion on the Energy Dissipation at Strength Strain. // Vestnik MGSU, No. 6. S. 26-34, 2016.
2. *Tamrazyan, A. G.* Recommendations for the Development of Requirements for the Durability of Buildings and Constructions. // Vestnik MGSU, No. 2. P. 77-83, 2011.
3. *Tamrazyan, A. G., Orlova, M. A.* To the Residual Load Bearing Capacity of Reinforced Concrete Beams with Cracks. // Housing, no. 6, Pp. 32-34, 2015.
4. *Tamrazyan, A. G.* Concrete and Reinforced Concrete – Glance at the Future. Tamrazyan, A. G. // Vestnik MGSU, No. 4. P. 181-189, 2014.
5. *Bondarenko, V. M., Klyueva, N. In., Piskunov, A. V.* Application of Dissipative Theory of Structural Safety of Reinforced Concrete // Proceedings of Orel GTU, Series Construction, Transport, № 1/21 (553), Pp. 8-19, 2009.
6. *Bondarenko, V. M.* The Specificity of the Power of Resistance of Corroded Reinforced Concrete Structures and New Factors of Destruction // Proceedings of Orel GTU, Series Construction, Transport, № 4, Pp. 28-33, 2009.
7. SP 63.13330.2012. Concrete and Reinforced Concrete Structures.